

# Hidden Hyperuniformity in Soft Polymeric Materials

Alexandros Chremos<sup>1,\*</sup> and Jack F. Douglas<sup>1,†</sup>

<sup>1</sup>*Materials Science and Engineering Division, National Institute of Standards and Technology, Gaithersburg, MD, 20899, USA*

(Dated: January 28, 2019)

We investigate the nature of long-range density fluctuations in melts of model “soft” polymers, specifically stars and bottlebrushes, over a wide temperature range by molecular dynamics simulation. The cores of the stars and the backbones of bottlebrush polymers are found to have a hyperuniform distribution, i.e., they exhibit anomalously small density fluctuations over a wide temperature range above the glass transition temperature. The hyperuniformity of these substituent polymer subregion is *hidden* since the fluid as a whole does not exhibit this property. These findings offer a strategy for the practical design of hyperuniform polymeric materials.

Disordered hyperuniform materials arise from strong interparticle interactions that lead to particle localization and to a suppression of large scale density fluctuations, making these highly “jammed” materials useful in many applications in which low compressibility and material isotropy are required. In particular, hyperuniform materials have been observed to have enhanced fracture strength [1] and large *isotropic* photonic band gaps comparable to those of photonic crystals [2, 3]. Recent investigations have focused on the special mechanical [4], optical [5], photonic [6, 7], phononic [8], and transport properties of these materials [9]. However, design rules for the practical creation of hyperuniform materials have not yet been determined.

Density fluctuations are nearly completely suppressed in hyperuniform materials at large length scales, as quantified by the structure factor  $S(q)$  approaching zero in the limit  $q \rightarrow 0$ . Correspondingly, the fluid compressibility becomes small so that such materials are highly “jammed” and the direct correlation function, defined via the Ornstein-Zernike relation [10], is long-ranged [11]. Based on this definition, the “degree of hyperuniformity”  $h$  is defined as the ratio of  $S(0)$  over the value of  $S(q)$  at the first peak, which represents the average interparticle distance. Correspondingly, for a perfect hyperuniform material,  $h = 0$ , but more generally, a material at equilibrium is considered “effectively hyperuniform” if  $h$  satisfies the inequality  $h = S(0)/S_p < 10^{-3}$  [4, 12]. Classical fluids at their critical point also have a long-ranged density correlations, but  $S(q)$  diverges as  $q \rightarrow 0$  as the liquid transforms into a gas [13–15]. Characteristically, a fluid at its critical point becomes turbid in appearance due to the scattering of light by large scale density inhomogeneities [16]. Cooling liquids normally has the opposite effect, the amplitude of the density fluctuations leading to a  $S(0)$  decrease, in many cases resulting in optically transparent homogeneous solid materials in the form of crystals and glasses. While both perfect crystals and quasi-crystals at zero temperature are hyperuniform by definition, the degree of hyperuniformity  $h$  is sensitive to defects in the crystal structure and non-harmonic large scale thermal motion [12]. More-

over, the propagation of light in crystalline materials is anisotropic, which is a disadvantage in the use of isotropic thermal radiation sources [17] and waveguides with an arbitrary bending angle [18]. Glass-forming liquids are disordered systems that sometimes have high statistical isotropy and such materials have a smaller sensitivity to defects than crystals. However, near hyperuniformity is only found asymptotically as the temperature approaches the glass transition temperature,  $T_g$ ,  $h \gtrsim 10^{-3}$  [19–21]. The present work is concerned with how to achieve hyperuniform polymeric glass-forming materials.

We draw inspiration from already identified natural and synthetic hyperuniform materials, such as the photoreceptors of color-sensitive core cells in the eyes of certain birds [22], emulsified droplets [23], and the glassy minority blocks of sphere-forming block copolymers [24]. Additionally, we have observed [25] that fluids composed of nanoparticles with grafted polymers (PGNs) also exhibit a hyperuniform state of the core particles at temperatures well above  $T_g$ . The common feature of these materials is that they are composed of “soft” particles [26], meaning that the molecules/particles deform and overcome surface tension effects and/or applied stresses. These examples lead us to hypothesize that we may create hyperuniform configuration of particles by “dressing” the particle or molecule of interest by a soft layer that may deform to enhance the packing efficiency of the “composite” particles. In this Letter, we test this hypothesis by considering the core particles of star polymers and the backbone chains of bottlebrush polymers. We find that these grafted polymer layers can produce hyperuniform configurations of the star cores and backbone chains of the bottlebrush polymer as in the case of PGNs. Correlations between parts of the polymer are *hidden* when the local density correlations of all the particles are considered. Despite the hidden nature of the hyperuniformity, these materials can be harnessed for applications. In such cases, the core of star polymers and backbone chains of the bottlebrush polymers must have dielectric or mechanical properties that distinguish this part of polymer construct for these correlations to have observable consequences. We mention, for example, that backbone

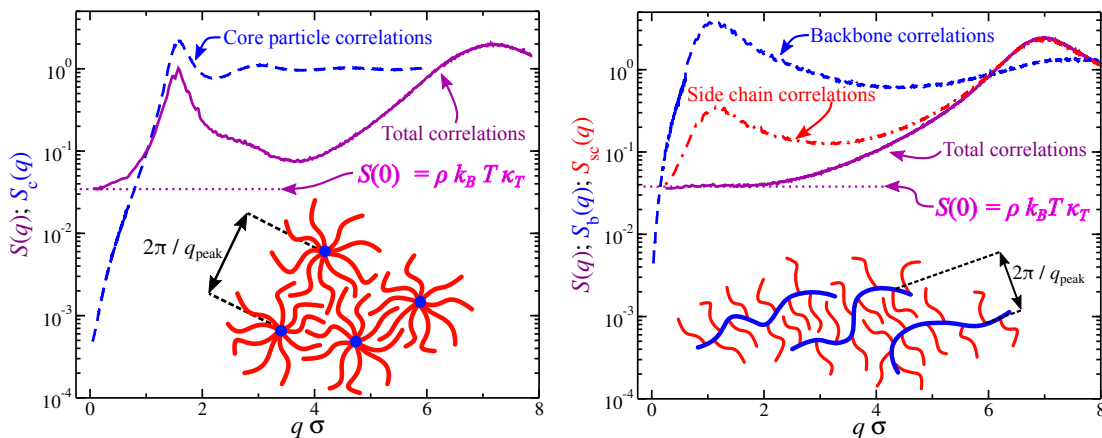


FIG. 1: Total static structure factor  $S(q)$  (continuous line) and partial structure factors of star and the bottlebrush polymer melts. The relation between the  $S(0) = \rho k_B T \kappa_T$  for  $S(q)$  and a schematic of the packing for bottlebrush and star polymers are also presented.

of bottlebrush polymers can be composed of conductive polymers [27, 28] and in the case of PGNs the core of the nanoparticles can be metallic, semiconducting, magnetic, etc. [29, 30], so that hyperuniform configurations of the core structures can be expected to be functional significant. In other words, we establish a general design rule for the development of hyperuniform materials.

Our polymer melts consist of  $N_p$  star or bottlebrush polymers. A bottlebrush polymer has a backbone chain composed of  $N_b$  segments and  $f$  side chains each composed of  $M$  segments, where one of their free ends is grafted along the backbone chain in a uniform fashion, i.e., one side chain per backbone segment. Thus, the total number of interaction centers per bottlebrush polymer is  $M_w = fM + N_b$ . A star polymer is effectively a bottlebrush having only one segment, i.e.,  $N_b = 1$ . Thus, the backbone becomes the core particle at which  $f$ -chains are grafted on its surface. The main focus of our current study is on the following set of parameters: star polymers having  $f = 16$  arms and  $M = 5$  segments per arm, bottlebrush polymers having arm lengths of  $M = 10$  segments, backbone lengths having  $N_b = 40$  segments, and grafting density,  $f/N_b = 1$ . The segmental interactions are described by the cut-and-shifted Lennard-Jones (LJ) potential with a cutoff distance  $r_c = 2.5\sigma$ , see Supplementary Information for more details. For all interactions,  $\varepsilon$  and  $\sigma$  define the units of energy and length. The segments along a chain are connected with their neighbors via a stiff harmonic spring,  $V_H(r) = k(r - l_0)^2$ , where  $l_0 = 0.99\sigma$  is the equilibrium length of the spring, and  $k = 2500\varepsilon/\sigma^2$  is the spring constant.

Simulations were performed in a cubic box with length  $L$ ; periodic boundary conditions were applied in all three directions. We utilized the large-scale atomic/molecular massively parallel simulator (LAMMPS) [31, 32]. Simulations were performed in the  $NVT$  ensemble after equi-

libration in the  $NPT$  ensemble at the desired temperature. Time averaging was conducted for  $O(10^8)$  time steps after equilibration with the time step set to  $\delta t = 0.005\tau$ , where  $\tau = \sigma(m_b/\varepsilon)^{1/2}$  is the unit of time. Temperature and pressure are measured in units of  $\varepsilon/k_B$  and  $\sigma^3/\varepsilon$ , respectively. Simulations were performed at different temperatures and  $\langle P \rangle \approx 0.1$  in reduced units.

We calculate the total structure factor  $S(q)$  of star polymer and bottlebrush polymer melts; see Fig. 1.  $S(q)$  of the entire bottlebrush polymer melt is similar to that of a simple liquid [10]. In both types of branched polymers, there is a peak in  $S(q)$  at  $q\sigma \approx 7$ , corresponding to the distance between the neighboring segments. For star polymers, there is an additional feature of a pre-peak associated with the higher in segmental density near the core particle [33]. Moreover, the density fluctuations are suppressed and a plateau is reached for  $q\sigma \lesssim 2$  for bottlebrush polymers and  $q\sigma \lesssim 0.3$  for star polymers. Based on this plateau position, one can reliably extrapolate to  $S(0)$ . For liquids in equilibrium, it is well known that  $S(0)$  and isothermal compressibility  $\kappa_T$  are related [10],

$$S(0) = \rho k_B T \kappa_T, \quad (1)$$

where  $\rho$  is the segmental density. The extrapolated values of  $S(0)$  from  $S(q)$  calculations are in agreement with the recently developed empirical correlation of volume  $V(T, P)$ , see Supplementary Information for more details, allowing the estimation of  $\rho$  and  $\kappa_T$ , via the Eq. 1, meaning that our systems are equilibrated. However, the hyperuniform parameter based on  $S(q)$  is larger than the threshold value  $h > 10^{-3}$ , suggesting that when these materials are considered as a whole then they are not effectively hyperuniform.

We next consider the partial static structure factor, corresponding to the backbone chain segments  $S_b(q)$  for bottlebrush polymers and core particles  $S_c(q)$  of star

polymers; the latter is discussed in the Supplementary Information. For bottlebrush polymers, we find an additional peak in  $S_b(q)$ , which is absent in  $S(q)$ , near  $q\sigma \approx 1.1$  corresponding to the average distance between neighboring bottlebrush backbones, see Fig. 1. This is analogous to the pre-peak in  $S(q)$  in highly branched star polymers. Indeed, the pre-peak in the star polymers is also found in  $S_c(q)$  at the same location. Trends in the peak location and its scaling with molecular parameters is discussed in Ref. [34]. For smaller  $q$ -values, there is a steep decrease in  $S_b(q)$  and in  $S_c(q)$  as  $q \rightarrow 0$  and for low  $q$ -values  $S_b(q) < S(q)$ , as illustrated in Fig. 1. Interestingly, the location of the polymer peak or its height change little with  $T$  variation, as can be seen in Fig. 2. Specifically, the backbones lack short and medium range structural order, as illustrated for the intermolecular pair correlation function of backbone chains  $g_b(r)$  in the inset of Fig. 2. This lack of short and medium structural correlations makes the structure of the backbone chains less sensitive to  $T$  variation, which is also reminiscent of a gas [35]. The striking lack of medium range order in our case derives from strong shape-fluctuations of these polymers. Changes in  $S_b(q)$  are observed for  $q\sigma < 0.4$ , which we discuss below.

To probe the trends of the structural correlations as  $q \rightarrow 0$ , we prepared polymer melt systems having significantly more interaction centers than our original study (for star polymers from 32 400 to 20 250 000 and for bottlebrush polymers from 176 000 to 8 448 000 interaction

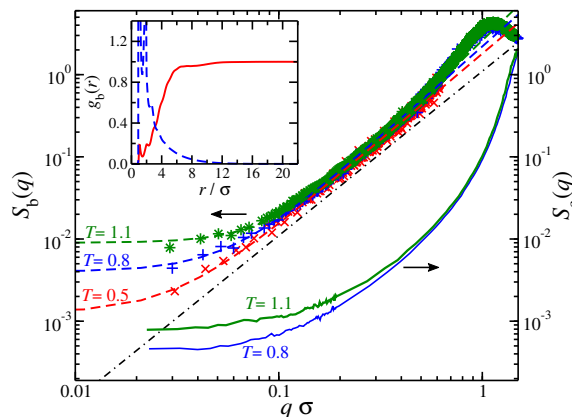


FIG. 2: Partial static structure factor of bottlebrush polymer melts, corresponding to backbone correlations  $S_b(q)$  (symbols), and of star polymers, corresponding to core particle correlations  $S_c(q)$  (continuous lines). Results for different temperatures are also presented. The dashed lines corresponds to fits based on a power law relation:  $S_b(q) = S_0(1 + cq^2)$ , where  $c$  and  $S_0$  are fitting parameters. The dot-dashed line corresponds to  $S_b(q) = 1.1q^2$ . Inset: Radial distribution function of the intra- and inter-backbone chains at  $T = 0.8$  represented by blue dashed line and continuous red line, respectively.

centers) [34]. The resulting  $S_b(q)$  curves at  $T > T_g$  are presented in Fig. 2. Star polymers reach a plateau at low  $q$ -values, a similar effect to that observed for bottlebrush polymers where  $S_b(q)$  monotonically decreases to smaller values as  $q \rightarrow 0$ . For both branched polymer types, the plateau in the partial correlations have small values, indicating that the density fluctuations of the backbone segments are significantly suppressed. This is understandable as the backbone chains in bottlebrush polymers, and correspondingly the core particle in star polymers, are localized by the surrounding grafted chains. When considering density correlations of the fluid as a whole, the lack of structural indicators of the strong suppression of the density correlations between the cores of the star polymers and the backbones of bottlebrush polymers suggests that these correlations are *hidden*. To obtain a better estimate of  $S_b(0)$  for bottlebrush polymers we note that  $S_b(q)$  seems to approach to a plateau at low  $q$  for  $T = 0.8$ , as in case of total structure factor  $S(q)$ , suggesting that  $S_b(q \rightarrow 0)$  reaches a non-zero plateau value  $S_0 > 0$ . We estimate  $S_0$  by fitting  $S_b(q)$  to the relation,  $S_b(q) = S_0(1 + cq^\alpha)$  in  $q\sigma < 0.4$ . We find the exponent is  $\alpha \approx 2$  so that  $S_b(q)$  consistent with the mean-field theory of critical fluids [14]. However, the constant  $c$  is positive as the hyperuniform limit is approached rather than negative as for fluids near their critical point. Negative  $c$  values are found in microemulsion materials [36, 37].

By combining an estimation of the partial structure factor as  $q \rightarrow 0$  and the height of the partial structure factor, we can determine the degree of hyperuniformity, see Fig. 3. The definition of  $h$  can be extended to non-equilibrium materials, so that the concept of hyperuniformity applies broadly to condensed materials [4]. For comparison, we also determine  $h$  for the whole polymer material based on  $S(q)$  for both star and bottlebrush polymer melts. It is evident that  $h$  is at least an order of magnitude smaller than when all the molecular segments are considered. The latter case closely tracks the  $h$  values for linear chain polymer melts; see Fig. 3. Moreover, the backbone chains exhibit  $h < 10^{-3}$  for  $T/T_g \lesssim 2$ , meaning that the backbone chains are effectively hyperuniform over a wide range of  $T$  over  $T_g$ . The degree of hyperuniform packing of the bottlebrush polymers is comparable with that of PGNs (Fig. 3). The core particles of star polymers exhibit even lower  $h$  values than both bottlebrush polymers and PGNs, even though the  $h$  values from the total correlations of star polymers is as linear chain polymer melts. Similar to bottlebrush backbones, the cores of star polymers are hyperuniform at temperatures well above  $T_g$ .

Recent work by the authors have demonstrated that suppression of density fluctuations in the backbones of bottlebrush polymer melts and in the cores of stars occurs over a wide range of molecular parameters, signifying a rather general trend [34]. Indeed, bottlebrush polymers and moderately branched star polymer melts

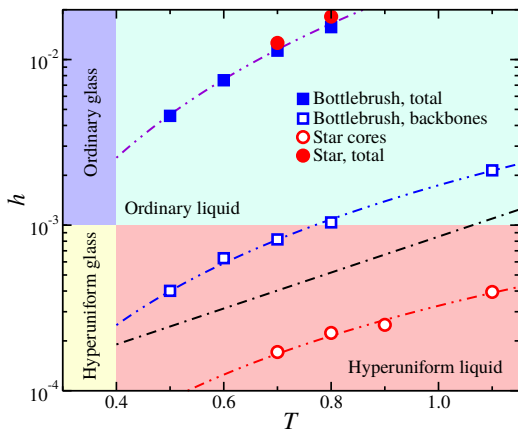


FIG. 3: Hyperuniformity parameter of bottlebrush polymer melts as a function of temperature,  $T$ . Results for total and backbone correlations are presented. The highlighted regions represent the regions at which glassy dynamics and the hyperuniform states emerge. The dot-dashed lines corresponds to  $h$ -parameter found for polymer grafted nanoparticles, for details see Ref. [25]. The double-dashed lines are based on power law relation  $h = cT^\delta$ , where  $c$  and  $\delta$  are fitting parameters; for the total correlation trends we utilize the parameters developed for linear chain melts  $(c, \delta) = (0.03, 2.69)$  and they are obtained in Ref. [20], while for the backbone trends we find  $(c, \delta) = (0.00174, 2.12)$  and for the core particles of star polymers we find  $(c, \delta) = (0.00033, 1.87)$ .

are more closely related in their configurational and thermodynamic properties, as well as to ring polymer melts, than linear chain melts [34, 38]. Similar suppression of density fluctuations has been observed in the packing of polymer-grafted nanoparticles in the absence of solvent, a novel type of materials that several studies demonstrated their have special properties related to hybrid character of the particles and the highly uniform packing configurations that these particles exhibit [39–41]. It is evident that branched molecules exhibit non-trivial correlations in their molecular packing and hyperuniformity can provide a valuable tool to probe these correlations.

Our observations of hyperuniformity in bottlebrush, star polymer melts, and previously in PGN melts [25], in conjunction with experimental observations of hyperuniformity in biological context (e.g., photoreceptors in the eye cells of certain birds [22]) and synthetic materials, e.g., sphere-forming block copolymers [24] and PGNs [30], indicate a general strategy for creating hyperuniform polymeric materials. Greater molecular packing efficiency is achieved by having one component fluid composed of molecules having a substituent of their particles (the core of the star polymers and PGNs or the backbone chains in the case of bottlebrush polymers) localized within their own molecular structure, which tends to increase the magnitude of  $S_p$  in the partial structure factor correlations. The combination of these features leads

to molecular packing that is highly uniform at *both* small and large length scales. An important practical consideration here is that the substituent particles can have different properties, such as being conductive [27, 28], to achieve useful property changes based on hyperuniformity, thus greatly expanding the usefulness of these materials. The cases of photoreceptors in the eye cells of certain birds [22] and the nuclei of cat retinal ganglion cells [42], can be considered to be, in a coarse-grained sense, like the cores of star polymers. We may also expect particles in plasmas [43, 44] and nanoparticles in ionic fluids [45] to interact through soft repulsive interactions, leading to hyperuniformity. Our findings offer a conceptual path for the design of hyperuniform polymer materials for many potential applications and provide scientific insight into the origin of this class of materials.

We gratefully acknowledge the support of the NIST Director’s Office through the NIST Fellows’ postdoctoral grants program. Official contribution of the U.S. National Institute of Standards and Technology – not subject to copyright in the United States.

\* Electronic mail: [alexandros.chremos@nist.gov](mailto:alexandros.chremos@nist.gov)

† Electronic mail: [jack.douglas@nist.gov](mailto:jack.douglas@nist.gov)

- [1] Y. Xu, S. Chen, P.-E. Chen, W. Xu, and Y. Jiao, Phys. Rev. E **96**, 043301 (2017).
- [2] M. Florescu, P. J. Steinhardt, and S. Torquato, Phys. Rev. B **87**, 165116 (2013).
- [3] W. Man, M. Florescu, E. P. Williamson, Y. He, S. R. Hashemizad, B. Y. Leung, D. R. Liner, S. Torquato, P. M. Chaikin, and P. J. Steinhardt, Proc. Natl. Acad. Sci. USA **110**, 15886 (2013).
- [4] S. Torquato, Phys. Rep. **745**, 1 (2018).
- [5] O. Leseur, R. Pierrat, and R. Carminati, Optica **3**, 763 (2016).
- [6] L. S. Froufe-Pérez, M. Engel, P. F. Damasceno, N. Müller, J. Haberko, S. C. Glotzer, and F. Scheffold, Phys. Rev. Lett. **117**, 053902 (2016).
- [7] L. S. Froufe-Pérez, M. Engel, J. José Sáenz, and F. Scheffold, Proc. Nat. Acad. Sci. **114**, 9570 (2017).
- [8] G. Gkantzounis, T. Amoah, and M. Florescu, Phys. Rev. B **95**, 258 (2017).
- [9] G. Zhang, F. H. Stillinger, and S. Torquato, J. Chem. Phys. **145**, 244109 (2016).
- [10] J.-P. Hansen and I. R. McDonald, *Theory of simple liquids* (Academic Press, Cambridge, 2006).
- [11] Y. Jiao, H. Berman, T.-R. Kiehl, and S. Torquato, PloS **6**, e27323 (2011).
- [12] J. Kim and S. Torquato, Phys. Rev. B **97**, 054105 (2018).
- [13] B. Widom, J. Chem. Phys. **43**, 3898 (1965).
- [14] H. E. Stanley, *Introduction to Phase Transitions and Critical Phenomena* (Oxford University Press, New York, 1971).
- [15] J. J. Binney, N. J. Dowrick, A. J. Fisher, and M. E. J. Newman, *The Theory of Critical Phenomena: An Introduction to the Renormalization Group* (Oxford University Press, Oxford, 1992).

- [16] V. G. Puglielli and N. C. Ford, Phys. Rev. Lett. **25**, 143 (1970).
- [17] M. Florescu, K. Busch, and J. P. Dowling, Phys. Rev. B **75**, 201101 (2007).
- [18] H. Miyazaki, M. Hase, H. T. Miyazaki, Y. Kurokawa, and Y. Shynya, Phys. Rev. B **67**, 1 (2003).
- [19] R. Xie, G. G. Long, S. J. Weigand, S. C. Moss, T. Carvalho, S. Roorda, M. Hejna, S. Torquato, and P. J. Steinhart, Proc. Natl. Acad. U.S.A. **110**, 13250 (2013).
- [20] W. S. Xu, J. F. Douglas, and K. F. Freed, Macromolecules **49**, 8341 (2016).
- [21] F. Martelli, S. Torquato, N. Giovambattista, and R. Car, Phys. Rev. Lett. **119**, 136002 (2017).
- [22] Y. Jiao, T. Lau, H. Hatzikirou, M. Meyer-Hermann, J. C. Corbo, and S. Torquato, Phys. Rev. E **89**, 022721 (2014).
- [23] J. H. Weijs, R. Jeanneret, R. Dreyfus, and D. Bartolo, Phys. Rev. Lett. **115**, 108301 (2015).
- [24] G. Zito, G. Rusciano, G. Pesce, A. Malafronte, R. Di Girolamo, G. Ausanio, A. Vecchione, and A. Sasso, Phys. Rev. E **92**, 050601 (2015).
- [25] A. Chremos and J. F. Douglas, Annalen der Physik **529**, 1600342 (2017).
- [26] C. N. Likos, Soft Matter **2**, 478 (2006).
- [27] P. Baek, N. Aydemir, Y. An, E. W. C. Chan, A. Sokolova, A. Nelson, J. P. Mata, D. McGillivray, D. Barker, and J. Travas-Sejdic, Chem. Mater. **29**, 8850 (2017).
- [28] S. E. Root, S. Savagatrup, A. D. Printz, D. Rodriguez, and D. J. Lipomi, Chem. Rev. **117**, 6467 (2017).
- [29] N. J. Fernandes, H. Koerner, E. P. Giannelis, and R. A. Vaia, MRS Commun. **3**, 13 (2013).
- [30] S. Srivastava, S. Choudhury, A. Agrawal, and L. A. Archer, Curr. Opin. Chem. Eng. **16**, 92 (2017).
- [31] S. J. Plimpton, J. Comput. Phys. **117**, 1 (1995).
- [32] *LAMMPS Molecular Dynamics Simulator*, URL <http://lammmps.sandia.gov/index.html>.
- [33] A. Chremos, E. Glynos, and P. F. Green, J. Chem. Phys. **142**, 044901 (2015).
- [34] A. Chremos and J. F. Douglas, J. Chem. Phys. **149**, 044904 (2018).
- [35] D. Bolmatov, V. V. Brazhin, Y. D. Fomin, V. N. Ryzhov, and K. Trachenko, J. Chem. Phys. **139**, 234501 (2013).
- [36] J. S. Huang, S. A. Safran, M. W. Kim, G. S. Grest, M. Kotlarchyk, and N. Quirke, Phys. Rev. Lett. **53**, 592 (1984).
- [37] S. T. Milner, S. A. Safran, D. Andelman, M. E. Cates, and D. Roux, Journal de Physique **49**, 1065 (1988).
- [38] A. Chremos and J. F. Douglas, J. Chem. Phys. **143**, 111104 (2015).
- [39] A. Chremos, A. Z. Panagiotopoulos, H.-Y. Yu, and D. L. Koch, J. Chem. Phys. **135**, 114901 (2011).
- [40] S. Srivastava, J. H. Shin, and L. A. Archer, Soft Matter **8**, 4097 (2012).
- [41] H.-Y. Yu, S. Srivastava, L. A. Archer, and D. L. Koch, Soft Matter **10**, 9120 (2014).
- [42] H. Wässle, L. Peichl, and B. B. Boycott, Nature **292**, 344 (1981).
- [43] M. Baus and J.-P. Hansen, Phys. Rep. **59**, 1 (1980).
- [44] E. Lomba, J.-J. Weis, and S. Torquato, Phys. Rev. E **96**, 062126 (2017).
- [45] K. Ueno and M. Watanabe, Langmuir **27**, 9105 (2011).

# Supplementary Information: Hidden Hyperuniformity in Soft Polymeric Materials

Alexandros Chremos\* and Jack F. Douglas†

Materials Science and Engineering Division, National Institute of Standards and Technology, Gaithersburg, MD, 20899, USA

## ADDITIONAL INFORMATION ON THE MODEL AND METHODS

We use a bead-spring model to model bottlebrush and regular star polymers. A bottlebrush polymer has a backbone chain composed of  $N_b$  segments and  $f$  side chains each composed of  $M$  segments, where one of their free ends is grafted along the backbone chain in a uniform fashion, i.e., one side chain per backbone segment, as illustrated in Fig. S1. A star polymer is effectively a bottlebrush having only one backbone segment, i.e.,  $N_b = 1$ . All the interactions in bottlebrush polymer melts are described by the cut-and-shifted Lennard-Jones (LJ) potential,

$$V(r) = \begin{cases} 4\varepsilon \left[ \left(\frac{\sigma}{r}\right)^{12} - \left(\frac{\sigma}{r}\right)^6 \right] - v & r \leq r_c \\ 0 & r > r_c \end{cases}, \quad (1)$$

where  $v$  is the value of the (unshifted) Lennard-Jones potential at  $r = r_c$ . The energy and length reduced units are  $\varepsilon$  and  $\sigma$  and the cutoff distance  $r_c = 2.5\sigma$ .

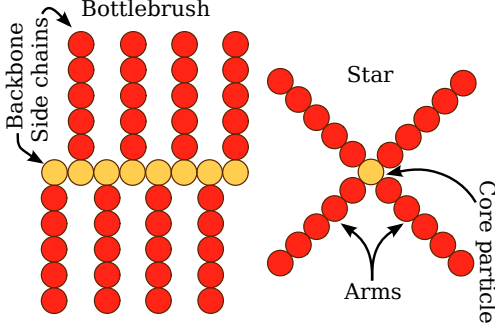


FIG. S1. Schematic illustration of the topological architecture of bottlebrushes and regular stars.

In the case of star polymers, all interactions are modeled by the LJ potential as in the case of bottlebrush polymers, except for the core particles where we use the purely repulsive Weeks-Chandler-Andersen potential [1] with modification taking into account the difference in the particle sizes [2],

$$V_{\text{WCA}}(r) = \begin{cases} 4\varepsilon \left[ \left(\frac{\sigma}{r-\Delta}\right)^{12} - \left(\frac{\sigma}{r-\Delta}\right)^6 + \frac{1}{4} \right] & r \leq r_m \\ 0 & r > r_m, \end{cases} \quad (2)$$

where  $r_m = 2^{1/6}\sigma + \Delta$ . The energy and interaction range parameters are chosen to be the same for interactions between core-core, core-segment, and segment-segment

such that  $\varepsilon_{\text{cc}} = \varepsilon_{\text{cb}} = \varepsilon_{\text{bb}} = \varepsilon$  and  $\sigma_{\text{cc}} = \sigma_{\text{cb}} = \sigma_{\text{bb}} = \sigma$ .  $\Delta = -0.5$  for core-core interactions and  $\Delta = -0.25$  for core-segment interactions.

## STATIC STRUCTURE FACTOR OF BOTTLEBRUSH POLYMER MELTS

We use two different approaches to estimate the structure factor  $S(q)$  of bottlebrush polymer melts at different temperatures as  $q \rightarrow 0$ . The first approach is a direct calculation of  $S(q)$ , where  $S(q)$  tends to have a linear dependence for  $q\sigma < 1$  and thus  $S(0)$  is extrapolated from this region. The second approach is by estimating  $S(0)$  from the equilibrium relation [3],

$$S(0) = \rho kT \kappa_T, \quad (3)$$

where  $\rho$  is the density,  $T$  is the temperature,  $k$  is the Boltzmann constant, and  $\kappa_T$  is the isothermal compressibility. The two main parameters that are needed are  $\rho$  and  $\kappa_T$  for the estimation of  $S(0)$  are estimated from an empirical relation that we have recently developed, see Ref. 4, and we briefly outline our approach below.

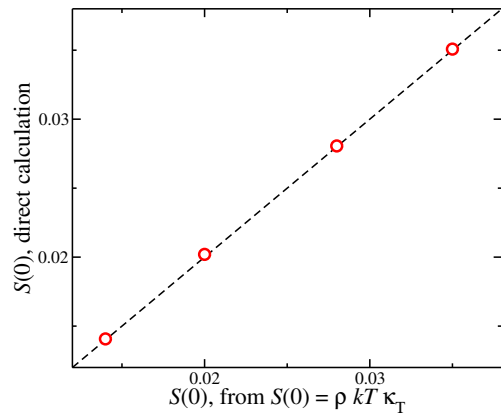


FIG. S2. Comparison of the total structure factor  $S(q)$  of bottlebrush polymers at different temperatures as  $q \rightarrow 0$  between two different approaches in calculating  $S(0)$ . The first approach is by extrapolation from the direct calculation of  $S(q)$  and the second way is by estimating  $S(0)$  from Eqn. 3, where  $\rho$  is the density,  $T$  is the temperature,  $k$  is the Boltzmann constant, and  $\kappa_T$  is the isothermal compressibility.

The volume  $V$  of the polymer melt is correlated as a function of  $T$  and pressure  $P$ ,

$$V(T, P) = -\frac{1}{2}k_2TP^2 - P(k_1T + k_3) + k_4T + k_5, \quad (4)$$

where  $k_1$ ,  $k_2$ ,  $k_3$ ,  $k_4$ , and  $k_5$  are fitting parameters. A series of simulations were performed at different pressures ( $P = 0, 0.05, 0.10, 0.15, 0.20$ , and  $0.25$ ) and temperatures ( $T = 0.55, 0.60, 0.65, 0.70$ , and  $0.75$ ) and the average volume was obtained. While these fitting parameters are system size dependent, the properties of interest to us, i.e.,  $\rho$  and  $\kappa_T$ , are not system size dependent in the  $T$  range of our investigation. We start by fitting the  $PVT$  data to Eq. 4 at  $P = 0$  and thus obtaining the  $k_4$  and  $k_5$  coefficients; note that  $k_4$  is  $\alpha_P V$  at  $P = 0$ . We then fit the  $PVT$  data to obtain the rest of the fitting parameters namely  $k_1$ ,  $k_2$ , and  $k_3$ . Once we have all the parameters, we obtain  $\rho$  and  $\kappa_T = -\frac{1}{V} \left( \frac{\partial V}{\partial P} \right)_T$  through differentiation of Eq. 4 at the desired thermo-

dynamic conditions within the boundaries of the fitting mentioned above.

The comparison between these two approaches is presented in Fig. S2, where each data point corresponds to a different temperature. The agreement between these two approaches means that our bottlebrush polymer melt systems are well equilibrated. Similar results are found for star polymer melts (not shown here).

---

\* Electronic mail: [alexandros.chremos@nist.gov](mailto:alexandros.chremos@nist.gov)

† Electronic mail: [jack.douglas@nist.gov](mailto:jack.douglas@nist.gov)

- [1] J. D. Weeks, D. Chandler, and H. C. Andersen, *J. Chem. Phys.* **54**, 5237 (1971).
- [2] J. S. Smith, D. Bedrov, and G. D. Smith, *Compos. Sci. Technol.* **63**, 1599 (2003).
- [3] J.-P. Hansen and I. R. McDonald, *Theory of simple liquids* (Academic Press, Cambridge, 2006).
- [4] A. Chremos and J. F. Douglas, *J. Chem. Phys.* **149**, 044904 (2018).